

**THD MITIGATION IN GRID-TIED SOLAR PV SYSTEM WITH THE MULTI-LEVEL
INVERTER AND MMPT BY THE ANN CONTROLLER**

S.Hussain Vali, Ginkala Karimulla, V.Rafi, Department of Electrical and Electronics Engineering
JNTUA College of Engineering Pulivendula, Kadapa, India.: vempallerafi@gmail.com

Abstract: This article presents a novel asymmetrical multilevel inverter topology for solar PV applications. The proposed topology achieves multi-level output voltage without H-bridge using asymmetric DC sources. This reduces the devices, cost, and size. The PV standalone system needs a constant DC voltage magnitude from the solar panels, maximum power point tracking (MPPT) technique is used for getting a stable output by using the ANN algorithm. This paper investigates artificial neural network (ANN) and DC-DC hybrid boost converter (HBC) based MPPT for improving the output power of solar plants. In this paper, a practical investigation of a Grid-Connected Photovoltaic System on the Total Harmonics Distortion (THD) on a sample low distribution network is applied to a case study tested with different loads.

I. Introduction

A few works have been carried out in the past years of research, on the standalone hybrid generation of systems using PV systems. Multilevel inverters are playing a wide role in the past few decades for high-power applications and DC-AC conversions. It started with three-level converters; numerous topologies were recently built for multilevel inverters [5]. To obtain high power a combination of switches in series and DC sources are used which produces a staircase voltage waveform. The DC sources may be anyone from renewable energy sources, batteries, capacitors, etc. Turning off and on the power, switches help to obtain the output stage at a high-level voltage for the multilevel inverter, where the switch voltage ratings depend on DC sources. The multilevel inverter has more benefits than a conventional two-level converter with Pulse Width Modulation (PWM) switching frequency. The various attributes include staircase waveform quality with minimum distortion, reduced dv/dt stresses that reduces the electromagnetic interferences (EMI). Common-mode (CM) voltage which produces stress in the bearings of a motor, removed using advanced techniques of modulation. A low distortion in multilevel inverters produce more input current. Multilevel inverter operates at fundamental frequency and at higher switching frequencies pulse width modulation [6]. Lower levels inverter in conventional method will not produce pure sinusoidal waveform resulting with high harmonics. Higher the voltage levels of inverter with high resolution, leads to sinusoidal waveform [7]. Based on the essential requirement of DC-AC inverter in a solar PV system, rather than the conventional inverters like voltage source inverter, multilevel inverter (MLI) has opted in the present scenario where it is efficient in capable of obtaining the quality of power with significantly less error [13]. The current multilevel inverter topologies comprise a smaller number of components used in the circuit compared with the conventional inverters such as flying capacitor type (FC) [14], cascaded H-bridge type (CHB) [15] and the neutral point clamped type (NPC) [16]. The number of components in the circuit is directly proportional to the number of levels in MLI, which increases cost and complex structure [17]. In both the FC MLI and NPC MLI, the capacitor voltage balancing is a challenging task with which these are limited to five-level and unable to cascade. This lowers the output voltage to half of the input voltage, providing high switching frequency with more losses [19]. A wide range of research is reducing the components of MLI, and several topologies are proposed based on the various levels which are having their challenges [20], [21]. Multilevel inverters are divided into isolated and non isolated. Isolated inverters are designed with external DC sources, whereas non-isolated inverters are designed with a single source [17]. Further, Isolated inverters are divided into symmetrical and asymmetrical configurations. Each DC source has an equal value known to be a symmetrical configuration, while different values of DC sources make up the asymmetrical design of MLI with trinary or binary techniques [18]. There are many such topologies which work for both configurations proposed in [23]. Specifically, for a photovoltaic power

generation under low and medium rated applications, the asymmetrical configuration is preferred, where the optimization of PV modules can be done quickly. In opting for the suitability among isolated and non-isolated structures, isolated MLI is optimal towards PV integration. In contrast, the non-isolated MLI like FC and NPC, the balancing of voltage is a challenging task [24]. Draw back such as electromagnetic interference and common mode voltage problems occur in conventional method which consumes high amount of current causing voltage swings. In televisions the rolling lines using inverters is a good example. A bridge inverter of single phase cascaded multilevel inverter is designed in series connection [9]. DC sources of the inverter generate different output voltages, +EDC, 0 and -EDC.

To date, soft computing techniques (SCT) are gradually becoming one of the practical and the suitable tool that supersedes the classical methods (Autoregressive Moving Average (ARMA) and Auto-regressive Method (AR)) [15- 17], for both online and offline PV forecasting, this is mainly due to their ability in solving non-linear and complex structure of big-data. From literature of SCT, many effectual methods (Artificial Neural Network (ANN), Support Vector Machine (SVM), and Fuzzy logic) can found in Refs. [18- 21]. One of the most powerful SCT used for RES forecasting is machine learning [18-20] and fuzzy logic [21, 22]. In this respect, artificial neural network (ANN) have been successfully employed for PV power output prediction (POP) [23-25]. In addition, Adaptive Neuro-Fuzzy Inference Systems (ANFIS) model, which combines the learning capability of ANN and the effective handling of imprecise information in fuzzy logic [26], have been applied to PV POP [27-34] immensely, due their good ability and performance for local linearization modeling. The active techniques of extracting maximum PV energy are still under development by exploiting the PV energy generation system and raising the competence of the power system to a particular level [17]. At present several algorithms have been developed for maximum power point tracking (MPPT). A few problems of the MPPT control approach are dealt with by adapting to the improvement of the intelligent optimization algorithm and combining it with the MPPT control approach [3]. Three general MPPT algorithms are a) hill-climbing search (HCS) or perturbation and observation (P&O), b) PV speed measurement (WSM), and c) power signal feedback (PSK) [7, 10]. Dissimilar computational intelligence (CI) methods, together with particle swarm optimization (PSO), mean-variance optimization (MVO), fuzzy logic, neural network, etc., have been used to deal with challenging control issues (both transient, dynamic, and steady-state controls) in WTG systems. P&O implementation is easy and also it leads to rapid convergence hence P&O has become popular for many applications [5]. The proposed strategy launched in this paper is the combination of P&O and ANN techniques. In Section 3, the PSO-ANN techniques are described. The performance results are analyzed in Section 4. Section 5 contains the concluding part of the paper.

II. MATHEMATICAL ANALYSIS OF PV SYSTEM

P-I Characteristic of a photovoltaic array Centralized inverter topologies are commonly employed in PV power generation systems due to their cost-effectiveness and ease of maintenance. A significant number of PV diodes are connected to an S-P arrangement. The output current of the PV panel can be expressed as [22]:

$$I = N_{PP}[I_{PV} - I_o(I_P - 2)] - \left(\frac{V + IR_s\tau}{R_p\tau}\right)$$

where

$$I = \exp\left(\frac{V + IR_s\tau}{V_T N_{SS}}\right) + \exp\left(\frac{V + IR_s\tau}{(P - 1)V_T N_{SS}}\right)$$
$$\tau = \frac{N_{SS}}{N_{PP}}$$

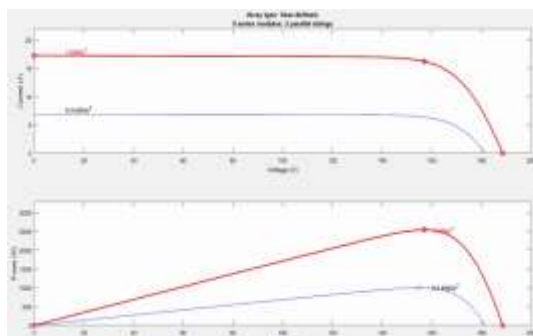


Fig1 V-I and P-V characters of the PV system.

Temperature Effects

With increasing temperature, the short-circuit current of the cell increases, whereas the open-circuit voltage decreases. The effect of temperature on PV power is quantitatively evaluated by examining the effects on the current and the voltage separately. Suppose I_o and V_o are the short-circuit current and the open-circuit voltage at the reference temperature T , and α and β are their respective temperature coefficients. If the operating temperature is increased by ΔT , then the new current and voltage are given by the following:

$$I_{sc} = I_o(1 + \alpha \cdot \Delta T) \text{ and } V_{oc} = V_o(1 - \beta \cdot \Delta T)$$

Because the operating current and the voltage change approximately in the same proportion as the short-circuit current and open-circuit voltage, respectively, the new power is as follows:

$$P = VI = I_o(1 + \alpha \cdot \Delta T) V_o(1 - \beta \cdot \Delta T)$$

This can be simplified in the following expression by ignoring a small term:

$$P = P_o[1 + (\alpha - \beta) \cdot \Delta T]$$

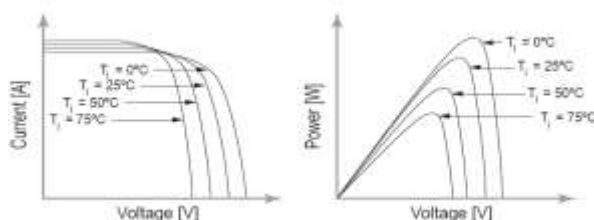


Fig 2 Effect of temperature on P-V characteristic

I and V are correspondingly, solar cell's output current and voltage V_t stands for the voltage of PV arrays, whereas I_{PV} is the photocurrent and I_0 the reverse saturation current of PV arrays. A series resistance is equal to R_S , while a parallel resistance equals R_P Photovoltaic (PV) cell production is highly connected to solar irradiance. The PV array has high nonlinear VI characteristics when solar irradiance fluctuates. As it does not have a constant voltage nor a constant current, it cannot supply a constant amount of electricity to a given load Most of the operating voltage range has a steady output current, but towards the open circuit voltage the current declines rapidly. It can be seen from the figure that the output characteristics of the photovoltaic array vary greatly under the influence of solar irradiance. When the solar irradiance increases, the output power increases.

Effect of Climate:

On a partly cloudy day, the PV module can produce up to 80% of its full sun power. It can produce about 30% power even with heavy clouds on an extremely overcast day. Snow does not usually collect on the module, because it is angled to catch the sun. If snow does collect, it quickly melts. Mechanically, the module is designed to withstand golf-ball-size hail.

FACTOR	SPECIFICATION
Location and Latitude	Coimbatore 11° 00' N
Day and Time	March 22, 14.30-15.30 (LST)

Average Intensity of solar radiation	560 W/m ²
Collector Tilt	26°
No. of glass cover	2
Heat Removal factor	0.82
Transmittance of glass	0.88
Absorptance of the plate	0.93
Top Loss coefficient (U _L)	7.95 W/m ²
Collector fluid temperature	75°C
Ambient temperature	25°C

TABLE 2.1: Data for a flat-plate collector used for heating

III. 31-level multilevel inverter

MLDCL inverter is a type of hybrid MLI inverter which consists of two stages. The first stage is the level generation part, where positive and zero voltage levels are generated to synthesize the waveform of stair-case output voltage. The second stage is the polarity generator part used to reproduce the second half-cycle of the generated waveform into negative levels. Figure 2 shows the circuit diagram of the 31-level asymmetric switch-diode based MLDCL inverter. For the asymmetrical operation of the MLDCL topology, it is more appropriate to use the binary source configuration where the voltage levels are determined by geometric progression (GP) with a factor of 2 [14]. Thus, in this paper, the voltage sources for the 31-level MLDCL are V_{DC}, 2V_{DC}, 4V_{DC}, and 8V_{DC}. The relationship can be given as:

$$\frac{V_{DC2}}{V_{DC1}} = \frac{V_{DC3}}{V_{DC2}} = \frac{V_{DC(n)}}{V_{DC(n-1)}} = 2$$

It is important to analyze the voltage across the switches and the peak inverse voltage VPIV of the diodes in order to select the most suitable components to be used. Selected devices for the implementation should have the maximum blocking voltage V_B and VPIV rating higher than the blocking voltage and VPIV measured. The blocking voltages of all the switches and PIV of all the diodes in this topology are given by:

$$V_{B,s1} = V_{PIV,D1} = V_{DC}$$

$$V_{B,s2} = V_{PIV,D2} = 2V_{DC}$$

$$V_{B,s3} = V_{PIV,D3} = 4V_{DC}$$

$$V_{B,s4} = V_{PIV,D4} = 8V_{DC}$$

$$V_{B,s5} = V_{B,s6} = V_{B,s7} = V_{B,s8} = 15V_{DC}$$

where V_{B,sn} is the blocking voltage of switch; and VPIV,D_n is the PIV of each diode. On the other hand, the maximum current I_m flowing through each switch or diode is the same as the load current I_{Load}, and it is zero when they are not conducting [31]. It can be given as:

$$I_{m,s1} = I_{m,D1} = \dots = I_{m,sn} = I_{m,Dn} = I_{Load}$$

where I_{m,sn} is the maximum current through the switch; and I_{m,Dn} is the maximum current through the diode. The switching states are the same for both half-cycles. The switching states at the polarity generation stage. The overview of the proposed standalone PV system is shown in Fig. 3, where PWM stands for pulse width modulation.

The proposed topology can be utilized for 31-level to generate AC waveform close to sine signal. The power switches of 31-level circuit are derived by the control circuit to form switching pulses as shown in Figure 8. The output voltage waveform in Figure 9 shows the operation of 31-level of the proposed topology. It is clearly shows that the operation of the circuit is obtained by the level generation and change polarity circuit to supply the AC signal to the load. The maximum value of the voltage stress was measured as 312 V for the input voltage $V = 20$ V. The peak-to-peak output voltage of the multilevel inverter across the load is varied from +185 to -185. It can be noticed that the output voltage is close to sine waveform.

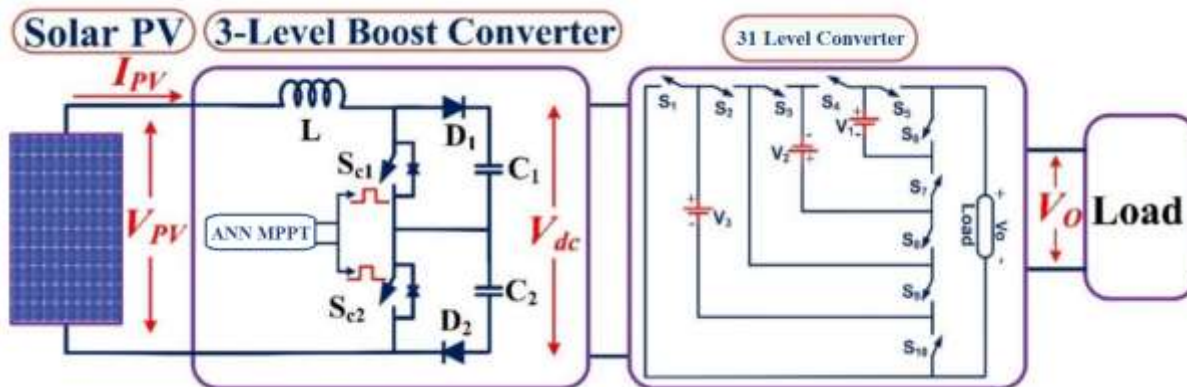


Fig3. Proposed Block diagram

IV. Proposed Algorithm

A hybrid control technique is proposed for tracking the maximum power generation system. The proposed hybrid controller is implemented in MATLAB/Simulink working platform. Here, the proposed controller is placed within the PWM inverter controller.

The P&O algorithm is used for calculating the dc-link reference voltage. The controlled signals are generated from the ANN technique. These signals are given to the inputs of the current controller which generates the controlling pulses.

V. BOOST CONVERTER

A boost converter is like a step-up chopper i.e., used to step up the input voltage level. The basic circuit diagram for a Boost regulator using IGBT, when the IGBT (Insulated gate bipolar transistor) is on current flows through the inductor and IGBT, and energy gets stored in the inductor. Now when IGBT is turned off then energy previously stored in the inductor is released through the capacitor and load. The amount by which the output voltage gets boosted depends upon the duty ratio.

$$\text{Duty ratio} = \frac{T_{ON}}{T_{ON} + T_{OFF}} k, \text{ and } V_o = \frac{V_{in}}{1-k} = \text{output voltage.}$$

VI. THE PROPOSED MPT METHOD FOR THE PMSGWTGS

ANN-Based MPPT Algorithm

The feed-forward ANN is meant to generate an MPPT connection with an enhanced converter controller and a favored pitch attitude to the pitch actuator based on the investigated function curves. In popularity, the structure of a multi-layer ANN accommodates enter, hidden, and output layers, as depicted in Fig6. The neurons of the hidden layers with proper weights and activation functions make sure that information flows from input neurons to output neurons.

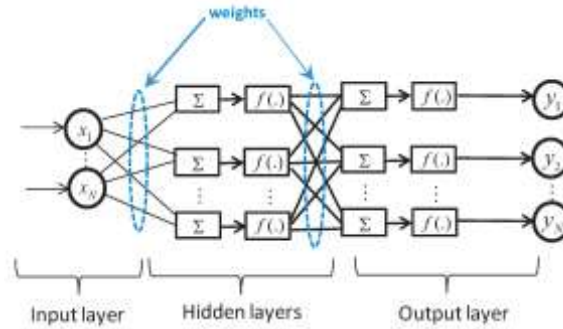


Fig4. ANN neural structure.

In order to create an ANN block, we should first configure the Solar PV input and output records. ANN block is educated to generate the right rotational speed reference by the use of the MPT method while maintaining the pitch angle null. When the Solar PV reaches its maximum power, the system should transfer to make certain the required pitch perspective for each input information on the way to keep away from the Solar PV from being overloaded. The constructed feed-forward community contains one enter layer with neurons representing tidal velocity fluctuations and one output layer with neurons.

This starts with a small wide variety of hidden neurons and increases the range of neurons. The neural network should then be taught and tested. The different types of hidden neurons are then raised, and previous layers are repeated until the training and checking of the outputs to obtain optimal values. The Levenberg–Marquardt (LM) set of rules is used for training the ANN as soon as the structure of neuro-controllers is adjusted[10]. LM set of rules is a variant of Newton's technique for decreasing capabilities which might be sums of squares of other nonlinear capabilities [11]. In order to minimize the overall performance index, the algorithm needs to update the network settings as follows [12]:

$$\text{Hessian matrix} = \nabla^2 F(X)$$

$$\Delta X = [\nabla^2 F(X)]^{-1} \nabla F(X) \tag{1}$$

$\nabla F(X)$ is a gradient.

Considering $F(X)$ as the current index,

It is defined as below:

$$F(X) = \sum_{i=1}^N e_i^2(X) = e^T(X) e(X) \tag{2}$$

The gradient may be given as:

$$\nabla F(X) = 2J^T(X)e(X) \tag{3}$$

Jacobian matrix = $J(X)$

Here the implementation of the LM method necessitates the construction of the Jacobian matrix with dimensions proportionate to a number of the training patterns[13].

Then, a Hessian matrix can be uttered in form of:

$$\nabla F(X) = 2J^T(X)J(X) + 2S(X) \tag{4}$$

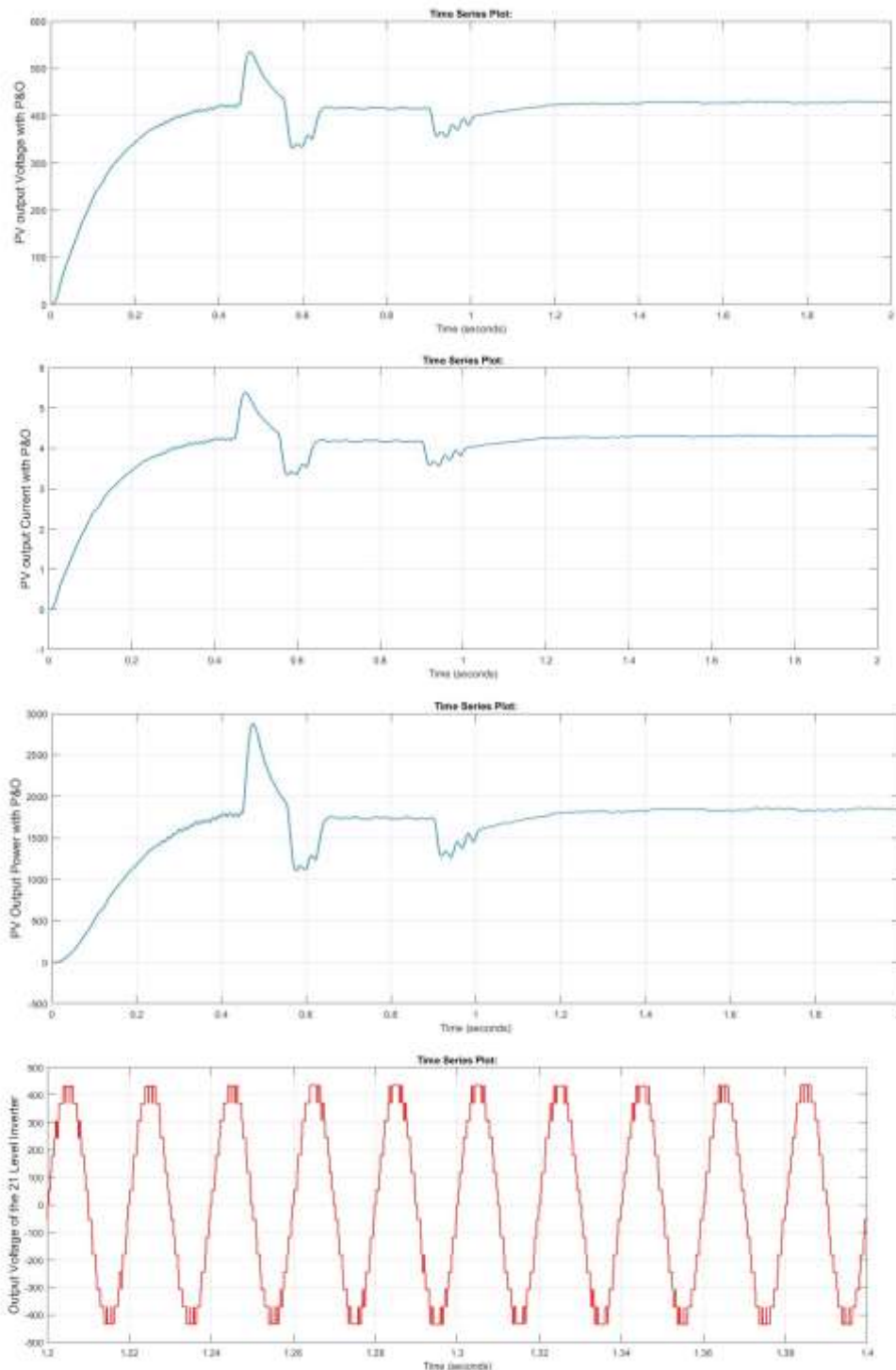
And

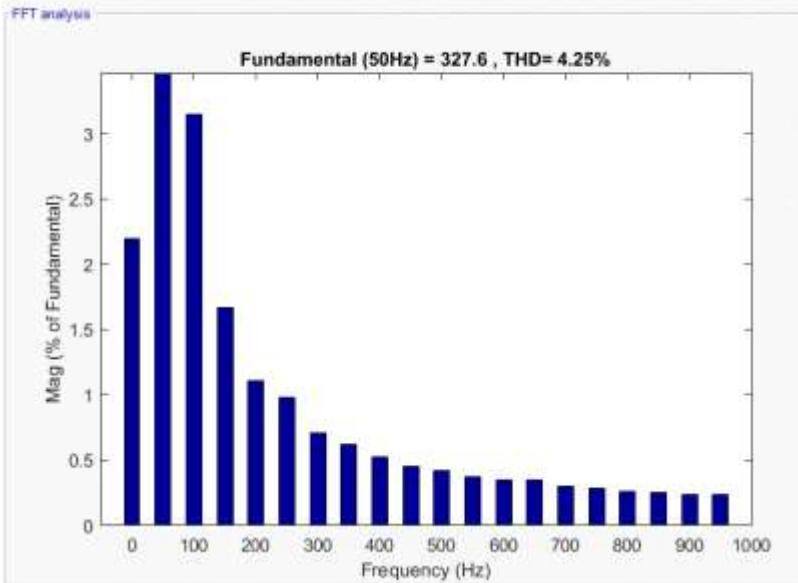
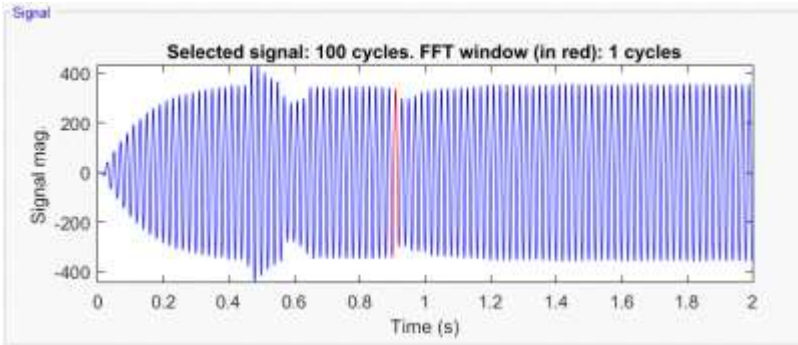
$$S(X) = \sum_{i=1}^N e_i(X) \nabla^2 e_i(X) \tag{5}$$

An empirical comparison analysis has achieved the use of numerous checks on the way to pick a sufficient number of neurons within the buried layer. The performance of the utilized LM technique

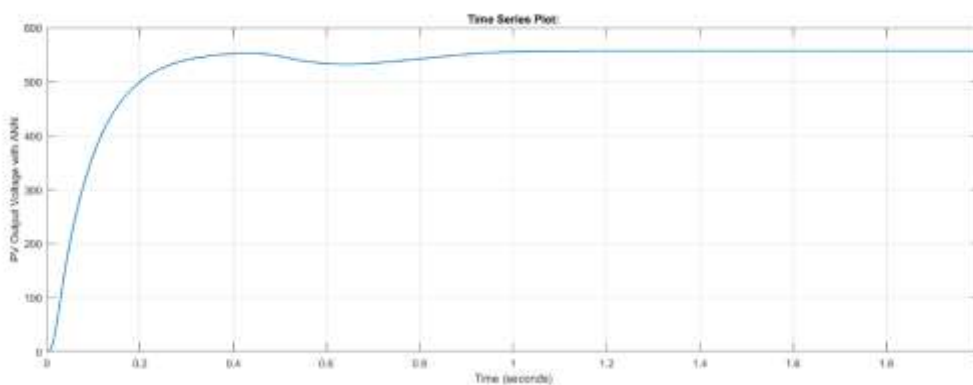
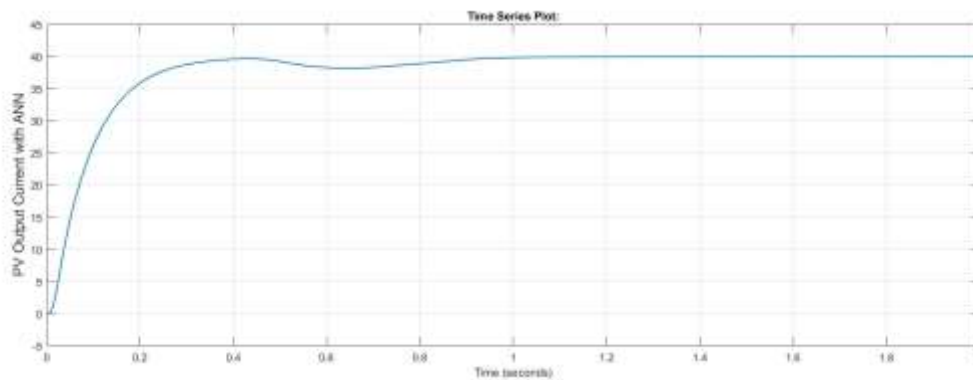
changed into evaluated via taking into consideration the number of epochs and simply squared mistakes determined. The education process's overall performance for varying numbers of neurons within a hidden layer. Training exams reveal ta hat growing wide variety of neurons inside the hidden layer permits LM algorithm to achieve a lower optimization preventing criterion across a greater wide variety of epochs. When hi is greater than 10, the MSE rises, indicating that network can be overtrained using such patterns.

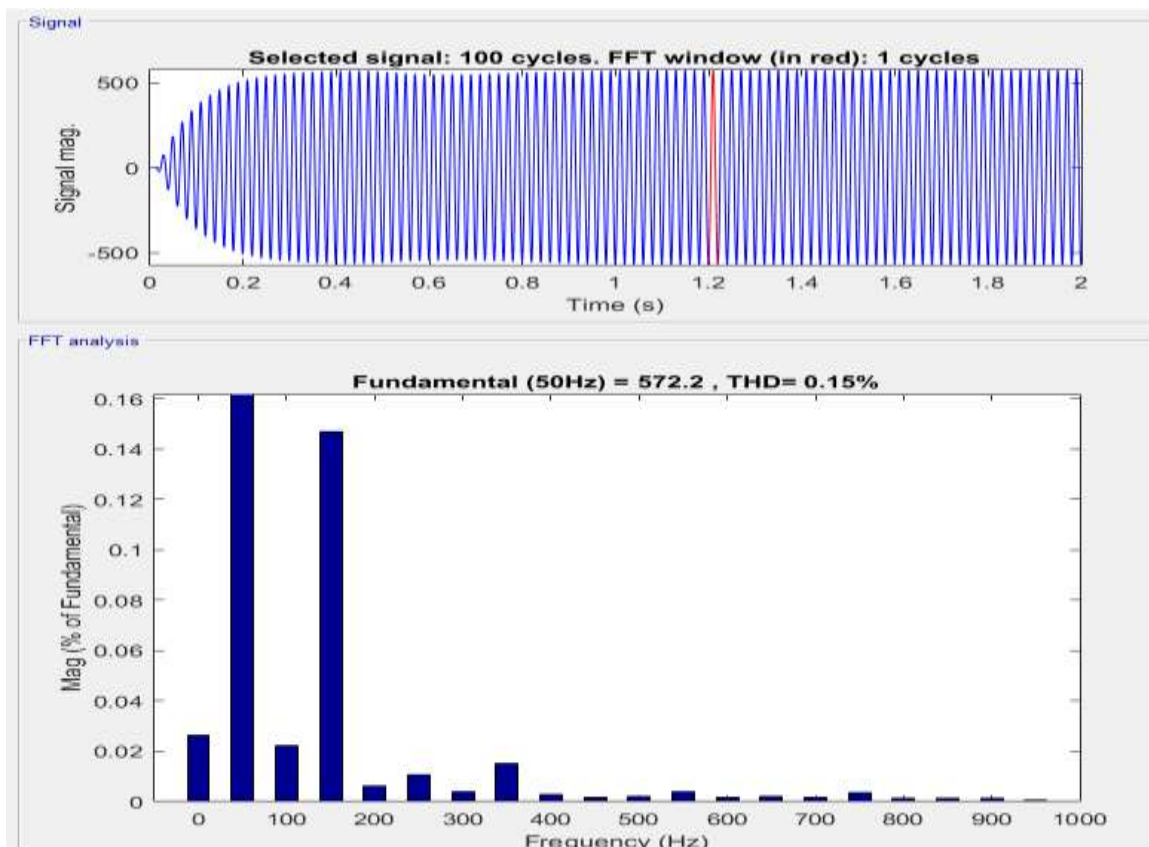
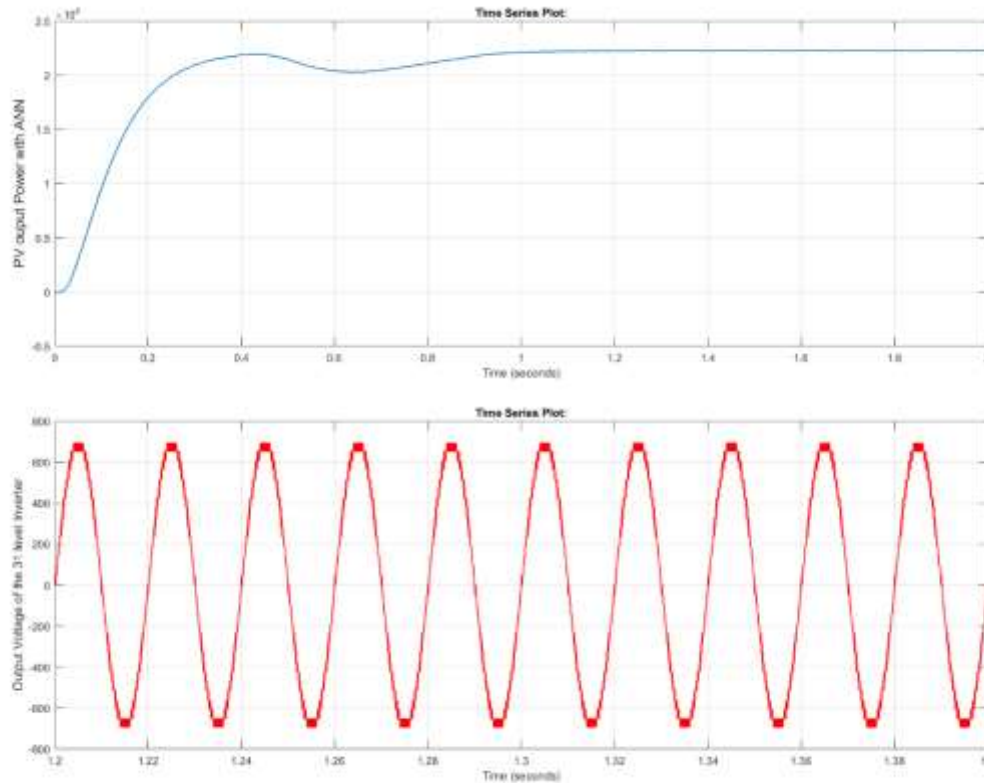
VII. Results **With P&O**





With ANN





Conclusion

This paper presented a proposed ANN-based MPPT method and multi-level inverter. The idea is a combination of those two methods. The ANN increases the tracking time of the PV by operating the DC-DC boost converter to MPPT. The proposed MLI requires fewer components to generate desired

output voltage levels with a low THD. The proposed MLI is tested under various dynamic load variations, and it is noticed that both simulation THD are 4.25% with the P&O 21 level MLI and the 0.15% with the ANN 31 level MLI. This shows the ANN 31 level MLI gives the better results compared to the P&O 21 level MLI.

References

- [1] N. A. Kamarzaman and C. W. Tan, "A comprehensive review of maximum power point tracking algorithms for photovoltaic systems," *Renew. Sustain. Energy Rev.*, vol. 37, pp. 585–598, Sep. 2014.
- [2] J. Macaulay and Z. Zhou, "A fuzzy logical-based variable step size P&O MPPT algorithm for photovoltaic system," *Energies*, vol. 11, no. 6, p. 1340, 2018.
- [3] M. Knez and B. Jereb, "Solar power plants—Alternative sustainable approach to greener environment: A case of Slovenia," *Sustain. Cities Soc.*, vol. 6, pp. 27–32, Feb. 2013.
- [4] A. R. Reisi, M. H. Moradi, and S. Jamasb, "Classification and comparison of maximum power point tracking techniques for the photovoltaic system: A review," *Renew. Sustain. Energy Rev.*, vol. 19, pp. 433–443, Mar. 2013.
- [5] G. Panayiotou, S. Kalogirou, and S. Tassou, "Design and simulation of a PV and a PV– PV standalone energy system to power a household application," *Renew. Energy*, vol. 37, no. 1, pp. 355–363, Jan. 2012.
- [6] A. S. Hassan, L. Cipcigan, and N. Jenkins, "Optimal battery storage operation for PV systems with tariff incentives," *Appl. Energy*, vol. 203, pp. 422–441, Oct. 2017.
- [7] E. E. A. Zahab, A. M. Zaki, and M. M. El-sotouhy, "Design and control of a standalone PV water pumping system," *J. Electr. Syst. Inf. Technol.*, vol. 4, no. 2, pp. 322–337, Sep. 2017.
- [8] S. Daher, J. Schmid, and F. L. M. Antunes, "Multilevel inverter topologies for stand-alone PV systems," *IEEE Trans. Ind. Electron.*, vol. 55, no. 7, pp. 2703–2712, Jul. 2008.
- [9] M. Mosa, M. B. Shadmand, R. S. Balog, and H. A. Rub, "Efficient maximum power point tracking using model predictive control for photovoltaic systems under dynamic weather conditions," *IET Renew. Power Gener.*, vol. 11, no. 11, pp. 1401–1409, Sep. 2017.
- [10] Y. Yang and H. Wen, "Adaptive perturb and observe maximum power point tracking with current predictive and decoupled power control for grid-connected photovoltaic inverters," *J. Mod. Power Syst. Clean Energy*, vol. 7, no. 2, pp. 422–432, Mar. 2019.
- [11] S. N. Singh, "Selection of non-isolated DC-DC converters for solar photovoltaic system," *Renew. Sustain. Energy Rev.*, vol. 76, pp. 1230–1247, Sep. 2017.
- [12] A. B. G. Bahgat, N. H. Helwa, G. E. Ahmad, and E. T. El Shenawy, "Maximum power point tracking controller for PV systems using neural networks," *Renew. Energy*, vol. 30, no. 8, pp. 1257–1268, Jul. 2005.